KINEMATIC ANALYSIS OF MECHANISM BY USING BOND-GRAPH LANGUAGE

Gregorio Romero, Jesús Félez, M. Luisa Martínez and Joaquín Maroto
Engineering Graphics and Simulation Group
Department of Mechanical and Manufacturing Engineering
Universidad Politécnica de Madrid
C\José Gutierrez Abascal Nº2, CP. 28006, Madrid (Spain)
E-mail:{gromero; jfelez; muneta; jmaroto}@etsii.upm.es

KEYWORDS

Bond Graph, differential, algebraic, equations, dynamics, kinematics, mechanism.

ABSTRACT

This paper presents a methodology for obtaining the equations corresponding to a mechanism that are necessary for carrying out a kinematic simulation. A simulation of this kind means obtaining the co-ordinates dependent on the system according to the movements imposed by the degrees of freedom. Unlike a dynamic simulation, where the set of elements moves according to the different external forces existing, in kinematic simulation the movement of the whole set depends exclusively on imposing movement on one or more of the bodies according to the degrees of freedom initially possessed by the mechanism. After presenting an analysis of how to obtain the necessary equations for several simple systems, this methodology is applied to the particular case of a wheel loader, where in order to move and tilt the bucket, various closed mechanisms are integrated.

1. INTRODUCTION

Real time simulation is an essential requirement in simulations such as those of vehicle dynamics, where the driver expects an immediate response, as is the case in a real situation. The implementation of each and every part of a vehicle, together with the fact that they are more and more complicated, means that this real time simulation requires a thorough in-depth analysis aimed at simplifying to the maximum everything that is either not strictly essential or requires more information than necessary.

When it comes to simulating machinery such as backhoes, wheel loaders,..., there are two parts that come together; that corresponding to the dynamics of the vehicle itself, and the part relative to the movement of implements such as bucket, arms, actuators, ...

The aim of this article is to demonstrate the validity of implementing the relevant kinematic equations corresponding to the bucket movement mechanism instead of dynamic equations. Thus, the set of equations needed to obtain the movement of the whole assembly, will depend solely on the movement of the main arms instead of on the external actions existing in all of the implements.

In recent years, the generation of dynamic equations of systems modeled with bond graphs has been the topic of considerable research. These equations have been presented in a variety of forms (Bos 1985). Classical formulations express these equations in terms of a large number of momentum associated to inertances and displacements associated to compliances. These elements can present integral or differential causality. In order to obtain these equations it is necessary to establish the causality in the model. Karnopp & Margolis (Karnopp and Margolis 1993) contributed with the stiff compliance approach, where high stiffness compliances are introduced in the model to eliminate the casual loops between integral and derivative causal storage ports. In this case, a set of differential equations is obtained, including as variables the flows associated to the previous inertances, displacements associated to the previous compliances, and the corresponding variables associated to the new stiff elements introduced, increasing seriously the number of differential equations to be solved. Usually, this approach needs the use of special numerical solvers for stiff differential equations, requiring very small integration step times. For these reasons, this procedure is not appropriate for simulation in real time.

Another approach was the introduction of Lagrange multipliers (Bos 1986) in the model. Some other authors (Gawthrop and Smith 1992) introduce residual sinks and sources ((Borutzky and Cellier 1996, Borutzky 1995) in a similar solution to the Lagrange approach (Félez et al. 1990). When Lagrange multipliers are used to break causal paths, a set of differential-algebraic equations is obtained, composed by a number of differential equations equal to the number of inertances plus compliances, and a number or algebraic (or constraint) equations equal to the number of Lagrange multipliers. The number of equations is the same than with the previous method, being also not appropriate for real time. Nevertheless, this approach presents important formulation advantages that will be

Proceedings 20th European Conference on Modelling and Simulation
Wolfgang Borutzky, Alessandra Orsoni, Richard Zobel © ECMS, 2006
ISBN 0-9553018-0-7 / ISBN 0-9553018-1-5 (CD)

considered in this work.

Previous methods prevent the existence of causal loops, but it is necessary to preanalyze the model and to modify the model in a subsequent operation (John D. et al. 1993). Another approach to solve the problem is the use of break variables (Félez et al. 1997, Félez et al. 2000) to open the causal loops. Causal loops always present an algebraic character. Algebraic loops relate their internal variables by means of algebraic relationships. It means that these kinds of loops do not involve integration operations. This fact leads to the definition of Zero-order Causal Paths ZCPs (Van Dijk and Breedveld 1991). The mathematical model obtained from bond graphs with ZCPs and opened with break variables is also a differential-algebraic equation set (DAE) (Romero et al. 2005, Granda 2005).

This last approach reduces the number of equations to a number equal to the number of inertances plus compliances plus break variables, but it is not enough for real time.

The use of Lagrange multipliers or the introduction of break variables implies the necessity of new variables and the appearance of constraint equations, increasing considerably the number of involved variables and the number of equations to be solved. These procedures are very useful to obtain the system equations in a systematic way, but they have to be improved or modified for their use in real time simulation.

2. SIMULATION OF MECHANISMS

As we know, kinematics studies the movements of particles and stiff bodies without taking account of the forces needed to give rise to these movements. Statics is the study of mechanical systems where the resultant of the system of forces is zero, and are thus balanced (at rest or moving at constant velocity). Finally, when this resultant is not zero, the mechanical system is charged with accelerated movement, and these unbalanced forces and the movements they give rise to, comprise the field of study called dynamics.

When it comes to studying a mechanism's movement, it is essential to choose one reference system or another. Thus, a system of local co-ordinates will usually be chosen when studying three-dimensional solids, which requires a change of reference systems in the existing joints of a mechanism of this type. When analysing the behaviour of a mechanism that only moves on a plane, it turns out to be much simpler to work with a system of co-ordinates that are parallel to the global system, which avoids having to change the reference systems in the joints.

When studying the movements of the different implements of an backhoe or wheel loader, it must be borne in mind that all of them move on a vertical plane, it being possible to study the corresponding flat mechanism. Therefore, the system of co-ordinates shown in the next figure, will be used.

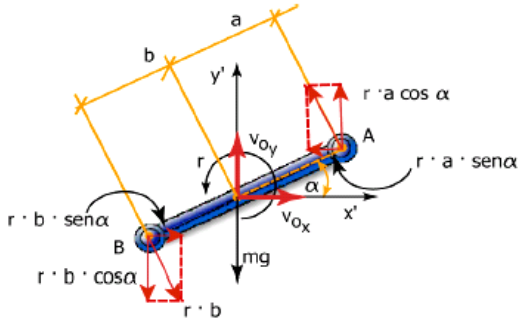

Figure 1. Planar 2D rod in global co-ordinates

The concept of degrees of freedom may be defined as the number of entries that need to be provided in order to give rise to a predictable exit. Each type of entry required will need some kind of starter or actuator, either in the form of a solenoid engine or hydraulic cylinder. Thus, a flat rod will consist of three degrees of freedom.

This is why a representation of a flat rod using a Bond-Graph will consist of three Inertial type ports (I_x, I_y and I_J).

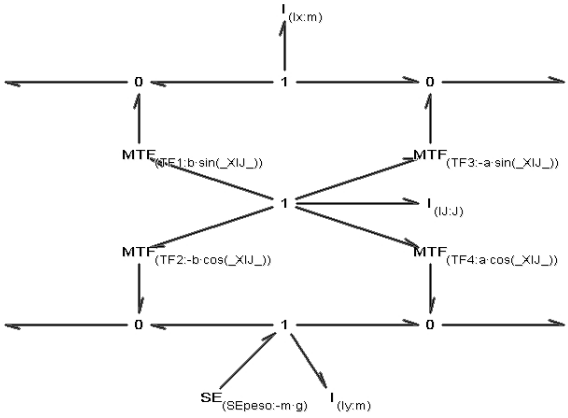

Figure 2. Planar 2D rod in global co-ords. using a Bond-Graph

In this figure we can see the name assigned to the element (*TF2*, *Ix*, …), two dots (:) and the expression associated to it (*-b·cos(_XIJ_)*, *m*, … respectively). The variables associated with the different ports are *P (m·V)* and *X* in the case of Inertances and Compliances respectively. If we write V_{I1}, we think in the velocity of a Inertance called *'I1'*, but in the case of the mechanism we need introduce the integral of V_{I1} into the *TF* elements, it said the angular displacement (X_{I1}). For this reason in the next examples I will use this notation to represent displacements (X_{Name}) and velocities (V_{Name}).

By way of example, we will study the behaviour of some simple mechanisms, with the aim of observing the differences existing as to the process for formulating movement equations depending on whether some

degrees of freedom are worked with rather than others, and how these equations are influenced by whether the mechanism under study is of an open kinematic chain, or to the contrary, contains some closed loop.
In order to analyse and study the equations corresponding to the use of the above Bond-Graph rod model , we will apply it to an open chain mechanism, as is the case of a double pendulum, and to two closed mechanisms, a crank-slider and an articulated quadrilateral. Finally, we will apply the results obtained to a wheel loader.

For the different examples presented the joints are assumed ideal.

3. DOUBLE PENDULUM

A double pendulum comprises two rods joined together, one of them being joined by a joint at a fixed point in space.

In an initial study, we will bear in mind that only the weight of both rods themselves act as external forces.

If we take what is shown in figure 2 as a rod model, the system formed using a Bond-Graph, once the causality has been obtained, will be as shown in the following figure.

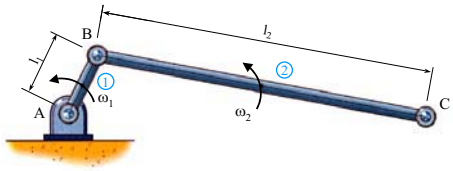

Figura 3. Double pendulum

As can be seen in the figure 4, there are only two degrees of freedom, those corresponding to each rod, (3x2) less the restrictions due to each joint (2x2).

The Compliances situated in the extreme of the model (*KptoC_x* and *KptoC_y*) are used to see the trajectory of the point C.

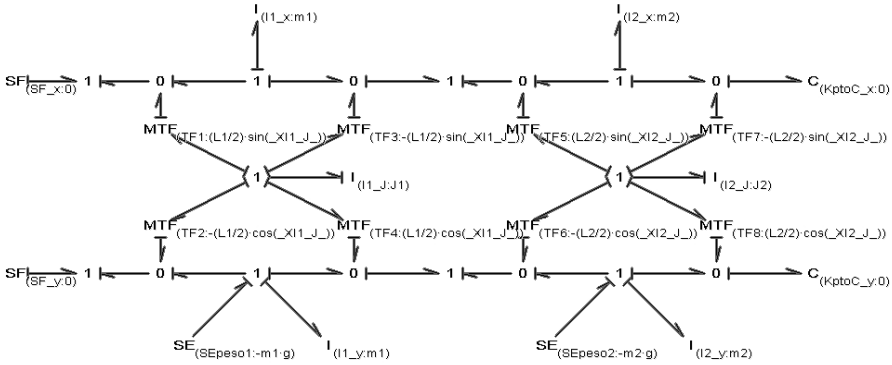

Figure 4. Double pendulum using Bond-Graph

Since the variables corresponding to the ports associated with the angular inertia of each rod, that is, the angular displacements, appear as parameters within the different transformer elements, these ports must be the ones that correspond to the degrees of freedom, and thus, have integral causality.

There are therefore 2 ports with integral causality and 4 with differential causality, which means that the system of equations corresponding to the double pendulum is formed by 2 differential equations and 4 algebraic ones in the following way:

$$\mathrm{VI1\_x}(t) = -\frac{1}{2} L1 \sin(\mathrm{XI1\_J}(t))\,\mathrm{VI1\_J}(t) \quad (1)$$

$$\mathrm{VI1\_y}(t) = \frac{1}{2} L1 \cos(\mathrm{XI1\_J}(t))\,\mathrm{VI1\_J}(t) \quad (2)$$

$$\mathrm{VI2\_x}(t) = -L1 \sin(\mathrm{XI1\_J}(t))\,\mathrm{VI1\_J}(t) - \frac{1}{2} L2 \sin(\mathrm{XI2\_J}(t))\,\mathrm{VI2\_J}(t) \quad (3)$$

$$\mathrm{VI2\_y}(t) = L1 \cos(\mathrm{XI1\_J}(t))\,\mathrm{VI1\_J}(t) + \frac{1}{2} L2 \cos(\mathrm{XI2\_J}(t))\,\mathrm{VI2\_J}(t) \quad (4)$$

$$\frac{d}{dt}\mathrm{VI1\_J}(t) = \frac{\left(m2\left(\frac{d}{dt}\mathrm{VI2\_x}(t)\right) + \frac{1}{2} m1\left(\frac{d}{dt}\mathrm{VI1\_x}(t)\right)\right) L1 \sin(\mathrm{XI1\_J}(t)) + \left(\left(-\frac{g}{2} - \frac{1}{2}\left(\frac{d}{dt}\mathrm{VI1\_y}(t)\right)\right) m1 + \left(-\left(\frac{d}{dt}\mathrm{VI2\_y}(t)\right) - g\right) m2\right) L1 \cos(\mathrm{XI1\_J}(t))}{J1} \quad (5)$$

$$\frac{d}{dt}\mathrm{VI2\_J}(t) = \frac{\frac{1}{2} m2\ L2 \sin(\mathrm{XI2\_J}(t))\left(\frac{d}{dt}\mathrm{VI2\_x}(t)\right) + \left(-\frac{g}{2} - \frac{1}{2}\left(\frac{d}{dt}\mathrm{VI2\_y}(t)\right)\right) m2\ L2 \cos(\mathrm{XI2\_J}(t))}{J2} \quad (6)$$

As can be seen, the equations (5)-(6) obtained depend on the external forces, which means that since they are not balanced, they will originate a movement and thus a dynamic simulation will be had.

However, if the angular variation experienced by each rod at a particular instant is introduced, that is, if movement is applied to as many elements as there are degrees of freedom initially existing, there will only be inertial ports with differential causality, as can be seen in following figure.

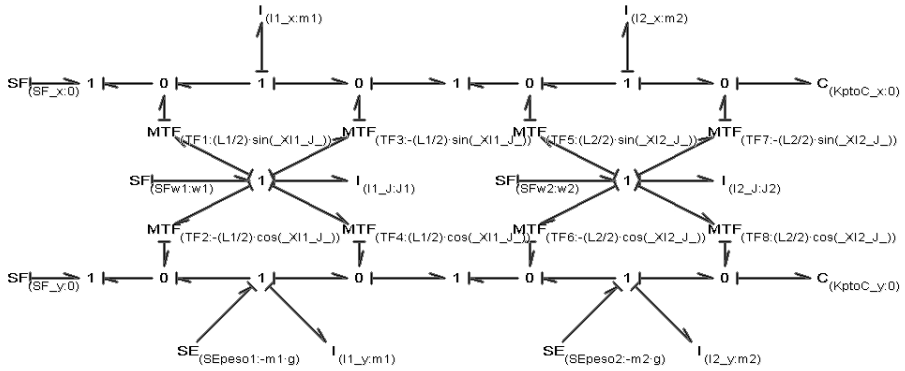

Figura 5. Double pendulum ω1 and ω2 using a Bond-Graph.

Once the differential algebraic equations have been obtained for the model (similar to eqs. (1)-(6)), it can be seen that the position of the different elements no longer depends on the external forces but only on the movements imposed and the geometric relationships existing between the two rods.

Reducing (Romero et al. 2005) the system of equations (1)-(6) to a differential one, we get:

$$\frac{d}{dt}\mathrm{XI1\_x}(t) = -\frac{1}{2} L1 \sin(\mathrm{XI1\_J}(t))\ \mathrm{w1}(t) \quad (7)$$

$$\frac{d}{dt}\mathrm{XI1\_J}(t) = \mathrm{w1}(t) \quad (8)$$

$$\frac{d}{dt}\mathrm{XI1\_y}(t) = \frac{1}{2} L1 \cos(\mathrm{XI1\_J}(t))\ \mathrm{w1}(t) \quad (9)$$

$$\frac{d}{dt}\mathrm{XI2\_x}(t) = -\frac{1}{2} L2 \sin(\mathrm{XI2\_J}(t))\ \mathrm{w2}(t) - L1 \sin(\mathrm{XI1\_J}(t))\ \mathrm{w1}(t) \quad (10)$$

$$\frac{d}{dt}\mathrm{XI2\_J}(t) = \mathrm{w2}(t) \quad (11)$$

$$\frac{d}{dt}\mathrm{XI2\_y}(t) = \frac{1}{2} L2 \cos(\mathrm{XI2\_J}(t))\ \mathrm{w2}(t) + L1 \cos(\mathrm{XI1\_J}(t))\ \mathrm{w1}(t) \quad (12)$$

As previously stated, kinematic simulation does not take account of the forces necessary to originate the movements of the different stiff bodies, as is the case here.

Thus, it may be stated that when dealing with a dynamic simulation where there are as many degrees of freedom initially as impositions of movement, it is possible to eliminate the inertial ports from the model along with the external forces.

Despite, if the same number of equations is to be formulated, they must be substituted by zero value compliance-type ports, obtaining a model similar to that shown in figure 6. We need add to the model a zero value port instead of null effort source because we need variables into the model (angle produced by the the two rods) and we cannot delete all the ports.

The difference between the original model and this one, is that although both systems generate the same final equations, the former starts from differential algebraic equations that have to be reduced to a system of differential equations, whereas since the latter has all the integral causality ports, the differential equations are obtained directly.

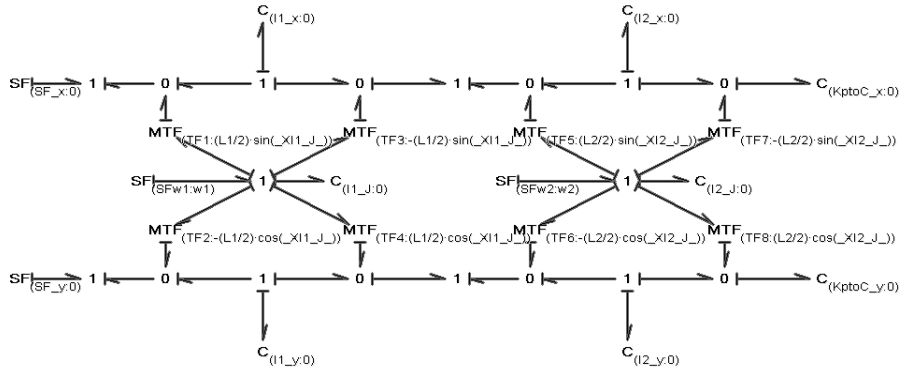

Figure 6. Double pendulum equivalent using a Bond-Graph.

Since the position of all the elements of the mechanism can be obtained by simply knowing the angles of each of the rods, the ports corresponding to the horizontal and vertical displacements can also be eliminated, thereby passing from an initial 6 differential algebraic equations (eqs. (7)-(12)) to 2 differential equations (eqs (8)-(11)).

Thus, the rod to be used in mechanisms having as many impositions of velocity as initial degrees of freedom, will contain only one zero value spring-type port.

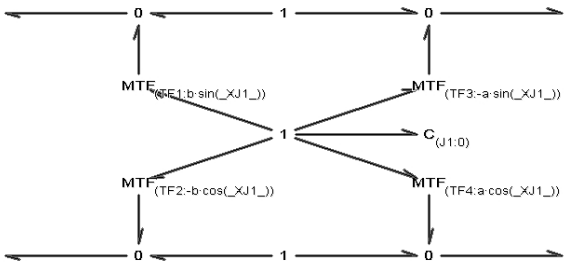

Figure 7. Flat rod equivalent using a Bond-Graph

4. CRANK-SLIDER MECHANISM

A mechanism of this kind is similar to the double pendulum dealt with in the above section, with the difference that the only end of the rods that was not restricted is only allowed movement in one direction here.

First, we will set out this mechanism in a Bond-Graph using flat rods in traditional global co-ordinates in order to obtain the corresponding equations and then we will do the same using the flat rod equivalent obtained in the section above.

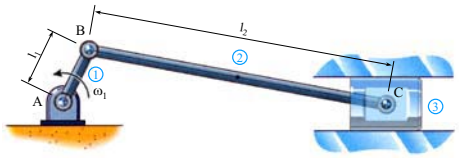

Figure 8. Crank-Slider mechanism

Unlike the previous model, this system comprises a closed mechanism, since we can pass from one element to another without twice passing over the same element on the ground. In this kind of element there exist fewer degrees of freedom than the number of rods.

As can be seen in the following figure, the model only has one degree of freedom, as many as correspond to each rod (3x2) less the restrictions due to each joint (2x2) and the one introduced at the very end of the rod nº 2 (1). So, by introducing a single velocity source, we can know the evolution of the rest of the model..

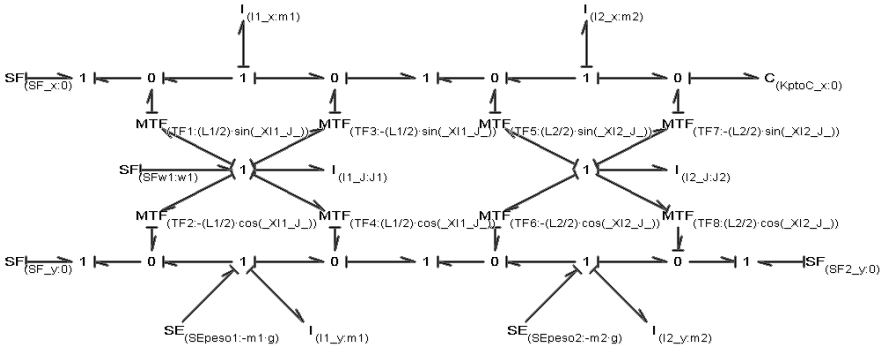

Figure 9. Crank-Slider mechanism using a Bond-Graph.

The introduction of this movement causes all the inertial-type ports to have differential causality, and makes it necessary to impose random causality on one of the intermediate graphs (*), and therefore, make up a set of differential algebraic equations (DAE):

$$Y1 = \frac{1}{2} L1 \cos(\mathrm{XI1\_J}(t))\ \mathrm{w1}(t) \tag{13}$$

$$Y2 = \frac{m2\ g}{2} \tag{14}$$

$$\frac{d}{dt}\mathrm{XI1\_x}(t) = -\frac{1}{2} L1 \sin(\mathrm{XI1\_J}(t))\ \mathrm{w1}(t) \tag{15}$$

$$\frac{d}{dt}\mathrm{XI1\_J}(t) = \mathrm{w1}(t) \tag{16}$$

$$\frac{d}{dt}\mathrm{XI1\_y}(t) = \frac{1}{2} L1 \cos(\mathrm{XI1\_J}(t))\ \mathrm{w1}(t) \tag{17}$$

$$\frac{d}{dt}\mathrm{XI2\_x}(t) = -L1 \sin(\mathrm{XI1\_J}(t))\ \mathrm{w1}(t) + \frac{\sin(\mathrm{XI2\_J}(t))\ Y1}{\cos(\mathrm{XI2\_J}(t))} \tag{18}$$

$$\frac{d}{dt}\mathrm{XI2\_J}(t) = -\frac{2\ Y1}{L2 \cos(\mathrm{XI2\_J}(t))} \tag{19}$$

$$\frac{d}{dt}\mathrm{XI2\_y}(t) = L1 \cos(\mathrm{XI1\_J}(t))\ \mathrm{w1}(t) - Y1 \tag{20}$$

In the previous equation´s system *Y1* and *Y2* dependent variables are the flow and effort associated with the intermediate graph (*) (Romero et al. 2005).

Working with the above system, we can form one made up of only differential equations (ODE), which makes it easier and quicker (sometimes) to solve:

$$\frac{d}{dt}\mathrm{XI1\_x}(t) = -\frac{1}{2} L1 \sin(\mathrm{XI1\_J}(t))\ \mathrm{w1}(t) \tag{21}$$

$$\frac{d}{dt}\mathrm{XI1\_J}(t) = \mathrm{w1}(t) \tag{22}$$

$$\frac{d}{dt}\mathrm{XI1\_y}(t) = \frac{1}{2} L1 \cos(\mathrm{XI1\_J}(t))\ \mathrm{w1}(t) \tag{23}$$

$$\frac{d}{dt}\mathrm{XI2\_x}(t) = \frac{-\frac{1}{4} L1\ \mathrm{w1}(t) \sin(\mathrm{XI1\_J}(t) + \mathrm{XI2\_J}(t)) - \frac{3}{4} L1\ \mathrm{w1}(t) \sin(\mathrm{XI1\_J}(t) - \mathrm{XI2\_J}(t))}{\cos(\mathrm{XI2\_J}(t))}$$

$$\frac{d}{dt}\mathrm{XI2\_J}(t) = -\frac{L1 \cos(\mathrm{XI1\_J}(t))\ \mathrm{w1}(t)}{L2 \cos(\mathrm{XI2\_J}(t))} \tag{25}$$

$$\frac{d}{dt}\mathrm{XI2\_y}(t) = \frac{1}{2} L1 \cos(\mathrm{XI1\_J}(t))\ \mathrm{w1}(t) \tag{26}$$

If we look closely at the initially formed DAE system (13)-(20), we can see how the term corresponding to the

weight of the second rod appears, while in the ODE system obtained (21)-(26) on reducing it, it does not appear. This shows that although the external force is included in the differential algebraic equations, it is really not necessary and in no way affects the final solution, whether it appears or not.

For this reason, since no external force influences the movement of the mechanism, it is possible to substitute the initial rods by those obtained in point 3, where only the ports corresponding to the angular displacement of the rods appear.

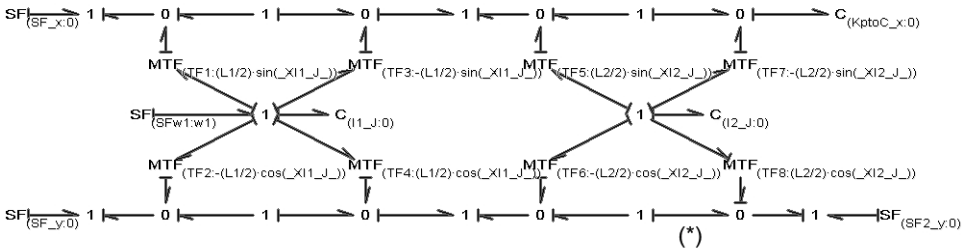

Figure 10. Crank-Slider mechanism equivalent using a Bond-Graph.

As with the initial model, causality needs to be imposed randomly on one of the intermediate graphs (*). To the contrary, all the ports that appear have integral causality and therefore the system of equations is formed by 1 algebraic equation and 2 differential equations instead of the previous 8 differential algebraic equations.

$$Y7 = \frac{1}{2} L1 \cos(\mathrm{XI1\_J}(t))\ \mathrm{w1}(t) \tag{27}$$

$$\frac{d}{dt}\mathrm{XI1\_J}(t) = \mathrm{w1}(t) \tag{28}$$

$$\frac{d}{dt}\mathrm{XI2\_J}(t) = -\frac{2\ Y7}{L2 \cos(\mathrm{XI2\_J}(t))} \tag{29}$$

Once the above equations have been operated with one other, it can be seen that the two differential equations thus formed (30),(31) correspond to those obtained on reducing the DAE system to ODE (22),(25), and therefore it can be concluded that both Bond-Graph models generate the same angular movement of the rods.

$$\frac{d}{dt}\mathrm{XI1\_J}(t) = \mathrm{w1}(t) \tag{30}$$

$$\frac{d}{dt}\mathrm{XI2\_J}(t) = -\frac{L1 \cos(\mathrm{XI1\_J}(t))\ \mathrm{w1}(t)}{L2 \cos(\mathrm{XI2\_J}(t))} \tag{31}$$

This same approach will be used for the following mechanism.

5. ARTICULATED QUADRILATERAL

An articulated quadrilateral is a mechanism where three rods are integrated by means of two joints, the remaining points being joined at fixed points in space.

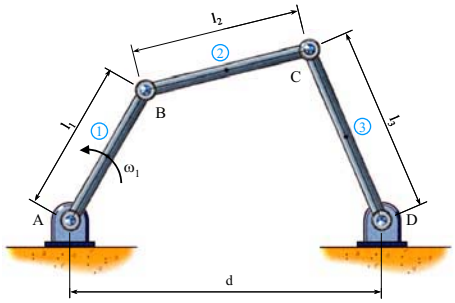

Figure 11. Articulated quadrilateral.

As before, we will make the initial approach with flat rods in global co-ordinates traditionally used in Bond-Graphs and then we will do so with the equivalent flat rods in question..

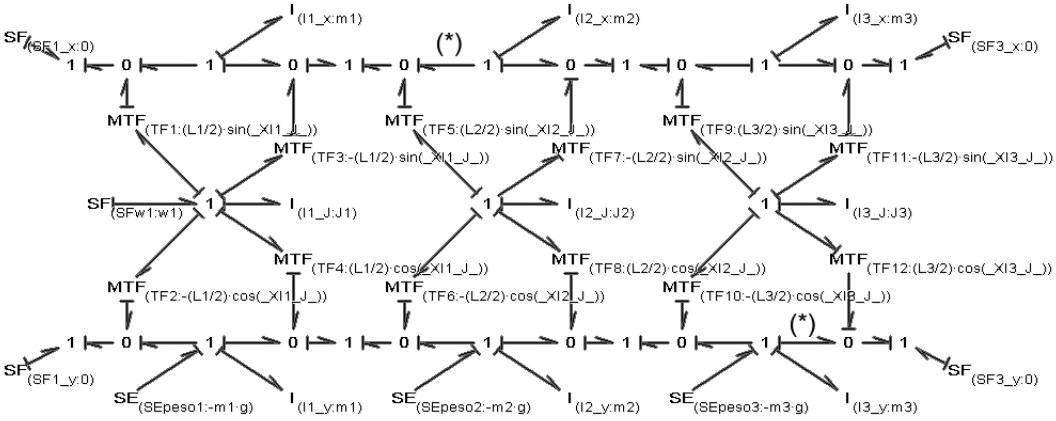

Figure 12. Articulated quadrilateral Bond-Graph.

There are three rods and four joints in this mechanism, which means the number of degrees of freedom will be one (3x3 - 4x2). As can be seen in the above figure, by introducing movement on one of the rods (rod 1), the movement for the rest of the model may be obtained.

In order to conclude the causal analysis of the model, random causality must be introduced on two of the intermediate graphs (*). It can be observed how all the ports have differential causality, for which reason, the corresponding system of equations will be of the differential algebraic kind (DAE):

$$Y0 = \frac{1}{4}\frac{-L1\ \mathrm{w1}(t)\cos(-\mathrm{XI1\_J}(t)+\mathrm{XI3\_J}(t)+\mathrm{XI2\_J}(t))-L1\ \mathrm{w1}(t)\cos(-\mathrm{XI1\_J}(t)+\mathrm{XI3\_J}(t)-\mathrm{XI2\_J}(t))+2\ L1\ \mathrm{w1}(t)\cos(\mathrm{XI1\_J}(t)+\mathrm{XI3\_J}(t)-\mathrm{XI2\_J}(t))}{\sin(\mathrm{XI3\_J}(t)-\mathrm{XI2\_J}(t))} \tag{32}$$

$$Y1 = \frac{(m3\ g+m2\ g)\,(\sin(-2\ \mathrm{XI2\_J}(t)+\mathrm{XI3\_J}(t))-\sin(2\ \mathrm{XI2\_J}(t)+\mathrm{XI3\_J}(t)))}{-4\cos(-2\ \mathrm{XI2\_J}(t)+\mathrm{XI3\_J}(t))+4\cos(\mathrm{XI3\_J}(t))} \tag{33}$$

$$Y2 = \frac{1}{4}\frac{L1\ \mathrm{w1}(t)\sin(\mathrm{XI1\_J}(t)+\mathrm{XI3\_J}(t)-\mathrm{XI2\_J}(t))-L1\ \mathrm{w1}(t)\sin(-\mathrm{XI1\_J}(t)+\mathrm{XI3\_J}(t)+\mathrm{XI2\_J}(t))}{\sin(\mathrm{XI3\_J}(t)-\mathrm{XI2\_J}(t))} \tag{34}$$

$$Y3 = \frac{3\ m3\ g}{4}+\frac{m2\ g}{4}+\frac{1}{4}\frac{(m3\ g+m2\ g)\sin(\mathrm{XI3\_J}(t)+\mathrm{XI2\_J}(t))}{\sin(\mathrm{XI3\_J}(t)-\mathrm{XI2\_J}(t))} \tag{35}$$

$$\frac{d}{dt}\mathrm{XI1\_x}(t) = -\frac{1}{2}L1\sin(\mathrm{XI1\_J}(t))\ \mathrm{w1}(t) \tag{36}$$

$$\frac{d}{dt}\mathrm{XI1\_J}(t) = \mathrm{w1}(t) \tag{37}$$

$$\frac{d}{dt}\mathrm{XI1\_y}(t) = \frac{1}{2}L1\cos(\mathrm{XI1\_J}(t))\ \mathrm{w1}(t) \tag{38}$$

$$\frac{d}{dt}\mathrm{XI2\_x}(t) = -L1\sin(\mathrm{XI1\_J}(t))\ \mathrm{w1}(t)-Y0-\frac{2\sin(\mathrm{XI3\_J}(t))\ Y2}{\cos(\mathrm{XI3\_J}(t))} \tag{39}$$

$$\frac{d}{dt}\mathrm{XI2\_J}(t) = \frac{2\ Y0}{L2\sin(\mathrm{XI2\_J}(t))}+\frac{4\sin(\mathrm{XI3\_J}(t))\ Y2}{\cos(\mathrm{XI3\_J}(t))\ L2\sin(\mathrm{XI2\_J}(t))} \tag{40}$$

$$\frac{d}{dt}\mathrm{XI2\_y}(t) = L1\cos(\mathrm{XI1\_J}(t))\ \mathrm{w1}(t)+\frac{\cos(\mathrm{XI2\_J}(t))\ Y0}{\sin(\mathrm{XI2\_J}(t))}+\frac{2\sin(\mathrm{XI3\_J}(t))\cos(\mathrm{XI2\_J}(t))\ Y2}{\cos(\mathrm{XI3\_J}(t))\sin(\mathrm{XI2\_J}(t))} \tag{41}$$

$$\frac{d}{dt}\mathrm{XI3\_x}(t) = -\frac{\sin(\mathrm{XI3\_J}(t))\ Y2}{\cos(\mathrm{XI3\_J}(t))} \tag{42}$$

$$\frac{d}{dt}\mathrm{XI3\_J}(t) = -\frac{2\ Y2}{L3\cos(\mathrm{XI3\_J}(t))} \tag{43}$$

$$\frac{d}{dt}\mathrm{XI3\_y}(t) = L1\cos(\mathrm{XI1\_J}(t))\ \mathrm{w1}(t)+\frac{2\cos(\mathrm{XI2\_J}(t))\ Y0}{\sin(\mathrm{XI2\_J}(t))}+\left(-1+\frac{4\sin(\mathrm{XI3\_J}(t))\cos(\mathrm{XI2\_J}(t))}{\cos(\mathrm{XI3\_J}(t))\sin(\mathrm{XI2\_J}(t))}\right)Y2 \tag{44}$$

As can be seen, the system of equations formed (32)-(44) is much more complex than for the previous model (13)-(20), without having introduced anything other than one rod and one restriction. As was to be expected, as the number of rods and restrictions increases, the system of equations formed is ever more complicated and tedious, which makes a real time simulation unapproachable.

On operating the different equations (32)-(44) with one another in order to get a system of differential equations, we obtain:

$$\frac{d}{dt}\mathrm{XI1\_x}(t) = -\frac{1}{2}L1\sin(\mathrm{XI1\_J}(t))\ \mathrm{w1}(t) \tag{45}$$

$$\frac{d}{dt}\mathrm{XI1\_J}(t) = \mathrm{w1}(t) \tag{46}$$

$$\frac{d}{dt}\mathrm{XI1\_y}(t) = \frac{1}{2}L1\cos(\mathrm{XI1\_J}(t))\ \mathrm{w1}(t) \tag{47}$$

$$\frac{d}{dt}\mathrm{XI2\_x}(t) = \frac{1}{4}\frac{(-\cos(-\mathrm{XI1\_J}(t)+\mathrm{XI3\_J}(t)+\mathrm{XI2\_J}(t))-\cos(-\mathrm{XI1\_J}(t)+\mathrm{XI3\_J}(t)-\mathrm{XI2\_J}(t))+2\cos(\mathrm{XI1\_J}(t)+\mathrm{XI3\_J}(t)-\mathrm{XI2\_J}(t)))\ \mathrm{w1}(t)\ L1}{\sin(\mathrm{XI3\_J}(t)-\mathrm{XI2\_J}(t))} \tag{48}$$

$$\frac{d}{dt}\mathrm{XI2\_J}(t) = -\frac{L1\sin(-\mathrm{XI1\_J}(t)+\mathrm{XI3\_J}(t))\ \mathrm{w1}(t)}{L2\sin(\mathrm{XI3\_J}(t)-\mathrm{XI2\_J}(t))} \tag{49}$$

$$\frac{d}{dt}\mathrm{XI2\_y}(t) = \frac{1}{4}\frac{(-\sin(-\mathrm{XI1\_J}(t)+\mathrm{XI3\_J}(t)+\mathrm{XI2\_J}(t))+2\sin(\mathrm{XI1\_J}(t)+\mathrm{XI3\_J}(t)-\mathrm{XI2\_J}(t))+\sin(-\mathrm{XI1\_J}(t)+\mathrm{XI3\_J}(t)-\mathrm{XI2\_J}(t)))\ \mathrm{w1}(t)\ L1}{\sin(\mathrm{XI3\_J}(t)-\mathrm{XI2\_J}(t))} \tag{50}$$

$$\frac{d}{dt}\mathrm{XI3\_x}(t) = \frac{1}{4}\frac{-L1\ \mathrm{w1}(t)\cos(-\mathrm{XI1\_J}(t)+\mathrm{XI3\_J}(t)+\mathrm{XI2\_J}(t))+L1\ \mathrm{w1}(t)\cos(\mathrm{XI1\_J}(t)+\mathrm{XI3\_J}(t)-\mathrm{XI2\_J}(t))}{\sin(\mathrm{XI3\_J}(t)-\mathrm{XI2\_J}(t))} \tag{51}$$

$$\frac{d}{dt}\mathrm{XI3\_J}(t) = -\frac{L1\sin(\mathrm{XI1\_J}(t)-\mathrm{XI2\_J}(t))\ \mathrm{w1}(t)}{L3\sin(\mathrm{XI3\_J}(t)-\mathrm{XI2\_J}(t))} \tag{52}$$

$$\frac{d}{dt}\mathrm{XI3\_y}(t) = \frac{1}{4}\frac{L1\ \mathrm{w1}(t)\sin(\mathrm{XI1\_J}(t)+\mathrm{XI3\_J}(t)-\mathrm{XI2\_J}(t))-L1\ \mathrm{w1}(t)\sin(-\mathrm{XI1\_J}(t)+\mathrm{XI3\_J}(t)+\mathrm{XI2\_J}(t))}{\sin(\mathrm{XI3\_J}(t)-\mathrm{XI2\_J}(t))} \tag{53}$$

If we apply the previously obtained rod equivalent, the model formed will only comprise spring ports with integral causality that will generate differential equations.

As with the traditional case, causality must be introduced on two of the intermediate graphs(*), which will generate algebraic equations.

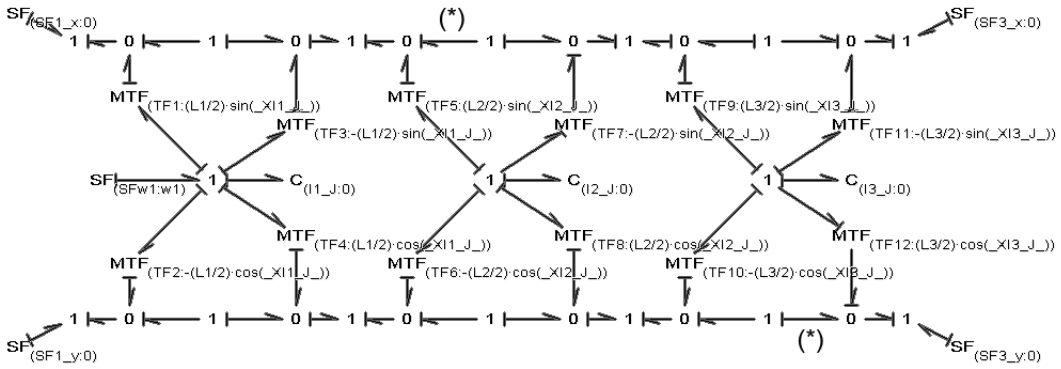

Figure 13. Articulated quadrilateral equivalent Bond-Graph.

The system of equations thus formed, will comprise two algebraic equations and three differential equations:

$$Y3 = \frac{1}{4}\,\frac{-L1\ \mathrm{w1}(t)\cos(-\mathrm{XI1\_J}(t)+\mathrm{XI3\_J}(t)+\mathrm{XI2\_J}(t)) - L1\ \mathrm{w1}(t)\cos(-\mathrm{XI1\_J}(t)+\mathrm{XI3\_J}(t)-\mathrm{XI2\_J}(t)) + 2\ L1\ \mathrm{w1}(t)\cos(\mathrm{XI1\_J}(t)+\mathrm{XI3\_J}(t)-\mathrm{XI2\_J}(t))}{\sin(\mathrm{XI3\_J}(t)-\mathrm{XI2\_J}(t))} \tag{54}$$

$$Y5 = \frac{1}{4}\,\frac{L1\ \mathrm{w1}(t)\sin(\mathrm{XI1\_J}(t)+\mathrm{XI3\_J}(t)-\mathrm{XI2\_J}(t)) - L1\ \mathrm{w1}(t)\sin(-\mathrm{XI1\_J}(t)+\mathrm{XI3\_J}(t)+\mathrm{XI2\_J}(t))}{\sin(\mathrm{XI3\_J}(t)-\mathrm{XI2\_J}(t))} \tag{55}$$

$$\frac{d}{dt}\mathrm{XI1\_J}(t) = \mathrm{w1}(t) \tag{56}$$

$$\frac{d}{dt}\mathrm{XI2\_J}(t) = \frac{4\ Y3\sin(\mathrm{XI3\_J}(t)+\mathrm{XI2\_J}(t)) - 4\ Y3\sin(\mathrm{XI3\_J}(t)-\mathrm{XI2\_J}(t)) + 8\ Y5\cos(\mathrm{XI3\_J}(t)-\mathrm{XI2\_J}(t)) - 8\ Y5\cos(\mathrm{XI3\_J}(t)+\mathrm{XI2\_J}(t))}{2\ L2\cos(\mathrm{XI3\_J}(t)) - L2\cos(2\ \mathrm{XI2\_J}(t)+\mathrm{XI3\_J}(t)) - L2\cos(-2\ \mathrm{XI2\_J}(t)+\mathrm{XI3\_J}(t))} \tag{57}$$

$$\frac{d}{dt}\mathrm{XI3\_J}(t) = -\frac{2\ Y5}{L3\cos(\mathrm{XI3\_J}(t))} \tag{58}$$

Operating the above equations with one another, we've:

$$\frac{d}{dt}\mathrm{XI1\_J}(t) = \mathrm{w1}(t) \tag{59}$$

$$\frac{d}{dt}\mathrm{XI2\_J}(t) = -\frac{L1\sin(-\mathrm{XI1\_J}(t)+\mathrm{XI3\_J}(t))\,\mathrm{w1}(t)}{L2\sin(\mathrm{XI3\_J}(t)-\mathrm{XI2\_J}(t))} \tag{60}$$

$$\frac{d}{dt}\mathrm{XI3\_J}(t) = -\frac{L1\sin(\mathrm{XI1\_J}(t)-\mathrm{XI2\_J}(t))\,\mathrm{w1}(t)}{L3\sin(\mathrm{XI3\_J}(t)-\mathrm{XI2\_J}(t))} \tag{61}$$

As we have seen, in these previous mechanisms, ones with as many velocity sources as initial degrees of freedom, the angular variation of each rod (59)-(61) may be obtained more quickly and effectively simply by using the rod in question, since the complexity and number of equations resulting from the model is reduced.

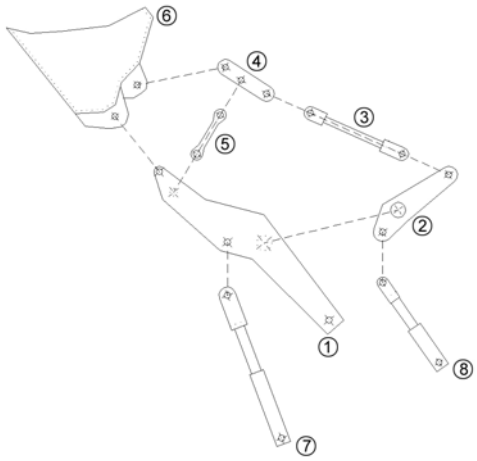

Figure 14. Wheel loader mechanism.

6. WHEEL LOADER MECHANISM

By using this mechanism, the raising and tilting movement of the bucket and the different arms that make it articulate, are obtained. They will be used to reproduce the movements of loading and unloading material, and will be formed by the arms, struts, bucket and actuators.

Movement of the different parts is performed by the action of two actuators (7 and 8) whose action will be implemented by introducing the movement corresponding to the support arm (1) or the tilt arm (2).

In order to form the Bond-Graph model for this mechanism, each of the elements of which it is made up will be started from in isolation, and after generating the Bond-Graph layout for each of them, they will be grouped and assembled.

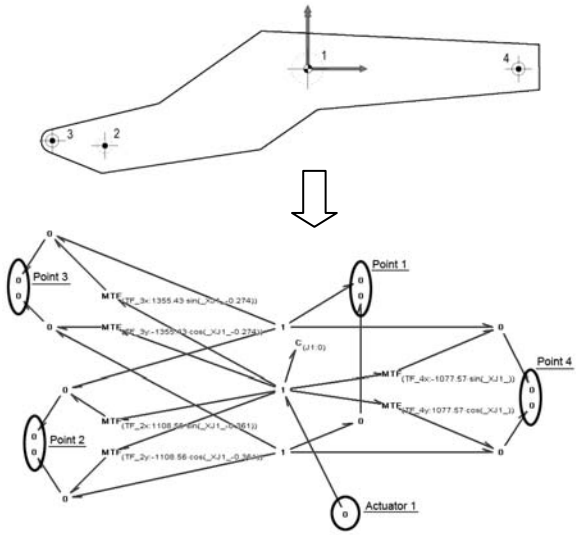

Figure 15. Support arm (element 1).

In order to facilitate assembly of all the elements once a Bond-Graph of one element has been made, their complete ports and nodes should be grouped and their entrances and exits left free so that the element can be linked to the rest of the subsets (fig. 16).

Once the different subsets of the mechanism have been obtained, it is essential to impose joints on the different nodes using restrictions, finally obtaining the mechanism we are dealing with.

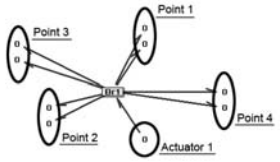

Figure 16. Support arm subset

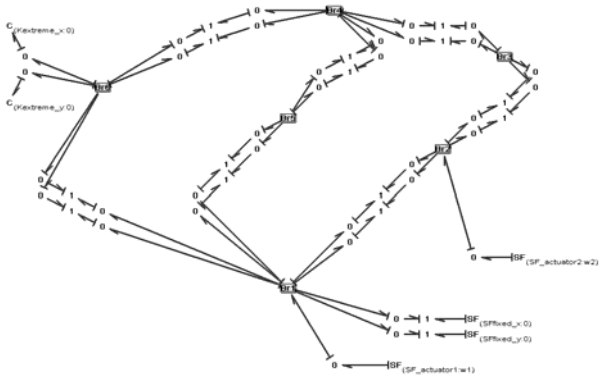

Figure 17. Wheel loader mechanism using a Bond-Graph.

In this way, the number of degrees of freedom will be proportional to the number of rods (6x3) and the restrictions due to joints (2x8). Thus it can be shown that there are only two degrees of freedom (6x3 – 2x8), as many as actuators, represented by ω1 and ω2.

After obtaining the differential equations corresponding to the model, the next step is to validate it using its numeric simulation.

The bucket movement consists of the alternate displacement of the two main arms, the support one (1) and the tilt one (2), so that starting from a state of rest the bucket will be placed horizontally at a small distance from the ground for it to be able pick up the load, raise it, and tilt in order to unload the material.

As we are dealing with a mechanism for moving the bucket, the movement and angle described by it will be represented during the simulation.

The following figure shows the phases comprising the bucket movement.

Firstly, starting from rest, the support arm (1) is initially lowered in order to move the bucket closer to the ground (A-B) and then this will be placed in a horizontal position (C-D) so that loading can be properly performed (D-E). Once material has been loaded, the bucket is tilted backwards (E-F) so that while circulating (F-G) with the bucket full, the material loaded does not fall out. Once the point for unloading the contents has been reached, firstly the arm is raised (G-H) and secondly, it is tilted forward (I-J), in order to unload the material. Finally, the bucket is tilted backwards (K-L), the arm lowered (M-N) and finally, the starting point returned to.

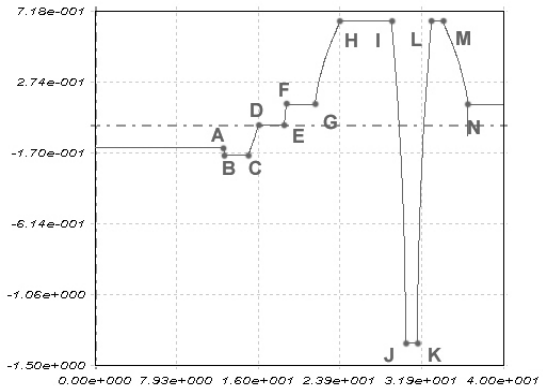

Figure 18. Bucket angle according to time

While the previous figure represents the resulting angle on the bucket produced by the combined movement of the actuators, the support one and the tilting one, the following figure shows the support arm angle.

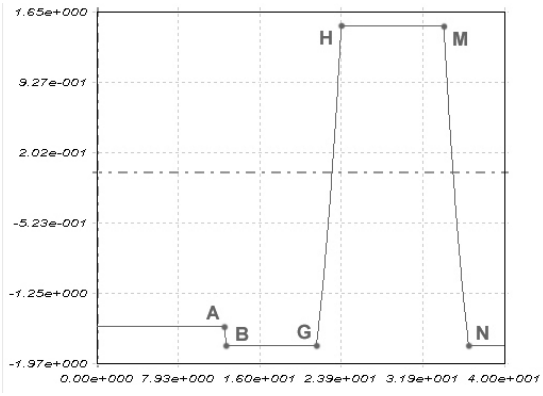

Figure 19. Support arm angle according to time

Finally, figure 20 shows the path drawn by the point situated at the end of the bucket.

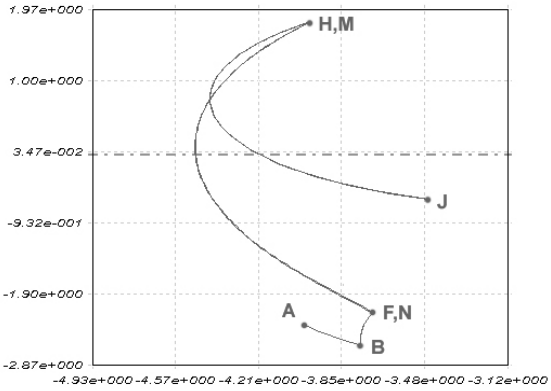

Figure 20. Path drawn by the end of the bucket

This figure shows how the end descends from its initial position (A) to a point located lower down (B), it is then tilted (F), partly to place the bucket horizontally, and partly to hold the material loaded. It is then raised in order to unload the bucket (H) and after tilting, it is moved to a point located lower down, (J). Once the material has been unloaded, the bucket returns to a position near to its original one after its tilting (M) and its descent (N).

7. CONCLUSIONS

Taking these results and those of the previous mechanisms as a basis, the advantage of setting out the elements using a Bond-Graph as presented here, stems from being able to set out the model, and thus the equations of a kinematic model, according to the displacements and angular velocities instead of the external forces. This makes it possible to find the equations typical of the model, not only in smaller number, but in less computation time needed to calculate them.

Although it is true that the problems of causal assignation will be the same in most cases, and it is necessary in both cases to assign random causality on intermediate graphs, thereby originating the same number of algebraic equations, in the way it is set out here, no more algebraic equations are added, as no differential causalities exist, and the number of variables and parameters needed are reduced by reducing the number of ports and because these are of zero value.

Finally, when dealing with mechanisms as complex as those of the wheel loaderl, the use of uncoupling elements is usually resorted to, which makes real time calculation unviable due to stiff behaviour. Should the solution to use stiff joints be adopted, the existence of three inertias with differential causality for each rod and the imposition of causality on intermediate graphs, makes calculation by DAE or ODE systems unapproachable, meaning that simulation is not possible.

8. BIBLIOGRAPHY

Bos, A.M. 1986. “Modeling Multibody Systems in terms of Multibond Graphs”. Ph. D. Thesis. Twente University, Enschede, The Netherlands.

Félez, J. et al. 1997. “Deriving simulation models from bond graphs with any combination of topological loop classes”. *International Conference on Bond Graph Modeling and Simulation ICBGM’97.* Phoenix. SCS Publishing, Simulation Series. Vol.29, No.1, pp.85-93.

Félez, J. et al. 2000. “Deriving simulation models from bond graphs with algebraic loops. The extension to multibond graph systems”. *Journal of the Franklin Institute.* Vol. 337 , pp.579-600.

Félez, J. et al. 1990. “Bondyn: A Bond Graph based simulation program”. *Trans. ASME. J. Dyn. Syst. Measurement and Control.* Vol.112 , pp.717-727.

Gawthrop, P.J. and Smith, L.S. 1992. “Causal augmentation of Bond Graphs with algebraic loops”. *J. of the Franklin Institute*. Vol. 329, No.2, pp.291-303.

Van Dijk, J. and Breedveld, P. 1991. “Simulation of system models containing Zero-order Causal Paths- I. Classification of Zero-order Causal Paths”. *J. of the Franklin Institute*. Vol.328, No.5/6, pp.959-979.

Karnopp, D.C. and Margolis, D.L. 1993. “Analysis and simulation of planar mechanism systems using Bond-Graph”. *J. of Mechanism Design*. Vol. 101, No.2,pp.187-191.

John D. Lamb et al. 1993. “Equivalences of bond graph junction structures”. *Intemational Conference on Bond Graph Modeling ICBOM'93*. San Diego. SCS Publishing, Simulation Series, Vol.25, No.2, pp.79-84.

Bos, A.M. 1985. “Implicit solutions to constraints in mechanical bond graphs”. *Proceedings IMACS Ist World Congress on Systems Simulation and Scientific Computation*. Oslo. Vol.4, pp.309-312.

Romero, G. et al. 2005. “Optimised procedures for obtaining the symbolic equations of a dynamic system by using the Bond-Graph technique”. *International Conference on Bond Graph Modeling and Simulation ICBGM’05.* New Orleans. SCS Publishing, Simulation Series. Vol.37, No.1, pp.51-58.

Romero, G. et al. 2005. “Systematic reduction of dynamic equations to a minimal set in systems modelled with Bond Graphs”. *International Conference on Integrated Modeling and Analysis in Applied Control* and Automation IMAACA’05. Marseille. pp.59-65.

Borutzky, W. and Cellier, F. 1996. “Tearing in Bond Graphs with Dependent Storage Elements”. Proceedings. of CESA'96, pp. 1113 - 1119

Borutzky, W. 1995. “Representing Discontinuities by Sinks of Fixed Causality”. *International Conference on Bond Graph Modeling and Simulation ICBGM’95*. pp. 65 – 72.

Granda, J.J. 2005. “The CAMP-G Symbolic Solution to Algebraic Loops in Bond Graph Models”. *International Conference on Bond Graph Modeling and Simulation ICBGM’05*. New Orleans. SCS Publishing, Simulation Series. Vol.37, No.1,

9. BIOGRAPHY

GREGORIO ROMERO received his Mechanical Engineering and Doctoral degrees from the UNED. (Spain) in 2000. He got his PhD Degree from the Politechnic University of Madrid in Spain in 2005 working on simulation and virtual reality, optimizing equations system. He has worked as Assistant Professor at the Technical University of Madrid in Spain (UPM) since 2001. He is developing his research in the field of simulation and virtual reality including simulation techniques based on bond graph methodology integrating computer graphics and virtual reality techniques to the simulation in real time. He has published over 20 technical papers and has been actively involved in over 11 research and development projects and different educational projects.

JESÚS FÉLEZ received his Mechanical Engineering and Doctoral degrees from the University of Zaragoza in 1985 and 1989. He started as Associate Professor at the Technical University of Madrid in Spain (UPM) in 1990 and became Full Professor in 1997. His main activities and research interests are mainly focused on the field of simulation, computer graphics and virtual reality. His research includes simulation techniques based on bond graph methodology integrating computer graphics and virtual reality techniques, mainly addressed towards the development of simulators. He has published over 50 technical papers and has been actively involved in over 25 research and development projects. He has served as thesis advisor for 30 master’s theses and four doctoral dissertations.

M. LUISA MARTÍNEZ received her Mechanical Engineering and Doctoral degrees from the Politechnic University of Madrid (Spain) in 1990. She got her PhD Degree in 1997 working on variational geometry. In 1990 she started to work as Associate Professor at the Technical University of Madrid in Spain (UPM). Her thesis was focused on variational geometry. She usually works in the field of computer graphics, virtual reality and CAD. During this time she has been involved in different educational projects and pilot activities promoted by the European Commission and other Spanish institutions. She has published over 23 technical papers and has been actively involved in over 16 research and development projects.

JOAQUÍN MAROTO received his Control Engineering and Doctoral degrees from the Madrid Polithecnic University in 2000 and 2005. He has been Assistant Professor at the Technical University of Madrid in Spain (UPM) since year 2003. His main activities and research interests are mainly focused on the field of simulation, computer graphics, virtual reality and machine vision. His main contribution is in the field of distributed virtual environment generation and ethe generation of immersive systems. He has published over 20 technical papers and has been actively involved in over 13 research and development projects.